PCCP

PAPER

View Article Online
View Journal | View Issue

Cite this: *Phys. Chem. Chem. Phys.*, 2018, **20**, 25096

Temperature dependence of photophysical properties of a dinuclear C^N-cyclometalated Pt(II) complex with an intimate Pt–Pt contact. Zero-field splitting and sub-state decay rates of the lowest triplet†

Joseph C. Deaton,[a] Arnab Chakraborty,[a] Rafal Czerwieniec,[b] Hartmut Yersin[b] and Felix N. Castellano*[a]

Received 15th August 2018,
Accepted 18th September 2018

DOI: 10.1039/c8cp05213a

rsc.li/pccp

The temperature dependence (1.7 K < T < 100 K) of emission decay is reported for the first time for a type of di-nuclear Pt complex featuring a metal–metal-to-ligand charge transfer (MMLCT) lowest energy transition that arises from a strong Pt–Pt interaction. The effect of local variation of the host/guest cage in a polymer matrix upon the phosphorescence decay time constants is characterized by the Kohlrausch–Williams–Watts function. The temperature dependence of the average decay time constants is fit by a Boltzmann-type expression to obtain the average zero-field splittings and individual sublevel decay rates of the photoluminescent triplet excited state.

Introduction

Luminescent Pt(II) complexes have emerged in many notable applications, including organic light-emitting diodes (OLEDs),[1–8] luminescent chemical sensors,[9–20] dye-sensitized solar cells,[21,22] photo-nanowires,[23] photon upconversion[24,25] photocatalysis,[26–32] biological imaging,[33–35] and photodynamic therapy.[36] Photophysical properties including emission energy, vibrational structure, and excited state lifetime afforded by Pt(II) complexes are highly varied dependent upon the nature of their electronic structure and bonding.[37]

One major class of phosphorescent Pt(II) complexes are the mononuclear cyclometalates.[38,39] As a result of numerous detailed studies of their spectroscopic and photophysical properties, the emissive state in these complexes has been assigned as dominantly ligand-centered (LC) π–π* having varied fractions of metal-to-ligand charge transfer (MLCT) character.[38–44] In cases of heteroleptic structures, the emissive state may have additional admixture of ligand-to-ligand charge transfer (LLCT) character. Due to the strongly σ-donating Pt–C bond, the cyclometalates typically exhibit more MLCT character, shorter radiative lifetimes, and superior photoluminescence quantum yields compared to analogous Pt(II) di- and tri-immine complexes; notable exceptions are when the latter contain ancillary carbon-donor ligands such as arylacetylides to supply additional electron density to the Pt center.[45–52]

Di-nuclear complexes composed of two d^8 ions where there is a strong interaction between the filled d_{z^2} orbitals and between the empty p_z orbitals from the two metal atoms often exhibit strong photoluminescence emission from state(s) resulting from low energy σ^* (d_{z^2}) → σ (p_z) excitation. The prototype of this class of emitters is $[Pt_2(\mu\text{-}P_2O_5H_2)_4]^{4-}$, abbreviated Pt(pop).[53–65] A highly unusual feature of this high symmetry (C_{4h} or approximate D_{4h}) complex is that both fluorescent and phosphorescent emission is observed. A derivative of the prototype that was structurally rigidized by BF_2 groups linking the diphosphonato ligands, $[Pt_2(\mu\text{-}P_2O_5(BF_2)_2)_4]^{4-}$, abbreviated Pt(pop-$BF_2$), exhibits the most outstanding photophysical properties of this genre with a combined fluorescence and phosphorescence quantum yield approaching 100%.[66–68] The lowest energy transition in these complexes involves a change in bond order, and indeed a shortening of the Pt–Pt distance in the excited state has been detected by time-resolved X-ray techniques.[69,70]

The subject of this contribution highlights a distinctly different class represented by a phosphorescent di-nuclear Pt(II) complex that comprises a chromophoric C^N-cyclometalating ligand on each Pt(II) atom that are bridged by bidentate ligands that secure the Pt atoms in position to interact through their d_{z^2} orbitals to form σ^* and σ levels (Fig. 1).[71–85] Through structural

[a] *Department of Chemistry, North Carolina State University, Raleigh, North Carolina, 27695-8204, USA. E-mail: fncastel@ncsu.edu*
[b] *Institut für Physikalische Chemie, Universität Regensburg, Universitätstrasse 31, D-93040 Regensburg, Germany*

† Electronic supplementary information (ESI) available: Additional temperature dependent photoluminescence spectra. See DOI: 10.1039/c8cp05213a

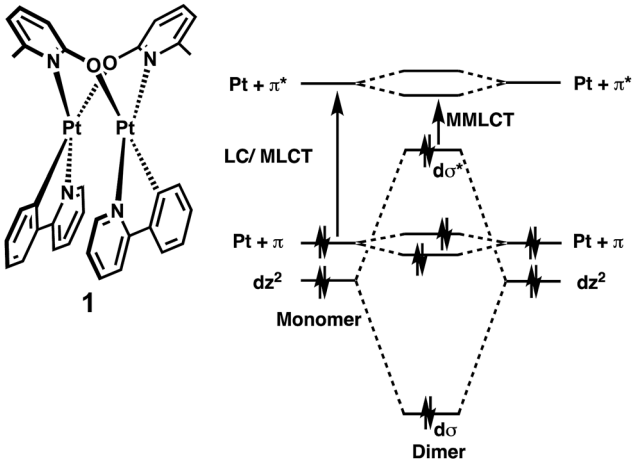

Fig. 1 Left: Chemical structure diagram of **1**. Right: Qualitative MO diagram illustrating the correlation from a mononuclear to a dinuclear cyclometalated complex having a strong Pt–Pt interaction.

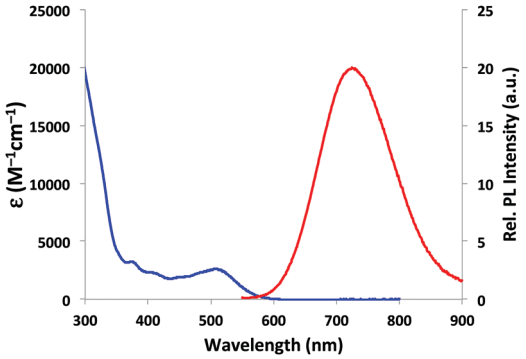

Fig. 2 Absorption (blue) and photoluminescence emission spectra (red) of **1** in deaerated THF.

variation of the bridging ligands, the nature of the photoluminescent state can be varied from predominantly LC in nature with some admixture of MLCT character, to strongly metal–metal-to-ligand charge transfer (MMLCT) in character wherein the originating orbital of the transition arises from the dσ* interaction between the Pt atoms.[71,72] These assignments were supported by correlations of trends in electrochemical oxidation potentials, spectral features, and photophysical properties, with the strength of the Pt–Pt interaction.[71–73] The assignment of MMLCT character in the emissive state of the complexes having the shorter Pt–Pt distances was additionally supported by TD-DFT calculations.[73] A contraction of the Pt–Pt distance in the excited state has been detected by time-resolved X-ray techniques for the latter complexes.[86,87] Vibrational coherence has been observed during the early time evolution of the excited state.[88]

The particular subject for the present investigation, *anti*-[Pt(ppy)(μ-(MepyO))]$_2$, (MepyO = 6-methyl-2-hydroxopyridine), **1**, was selected because it has one of the shortest Pt–Pt distances (2.82 Å) yet found for this class of chromophores, with only the benzoquinoline analog having a slightly shorter distance.[73] Pt–Pt distances may range up to 3.5 Å or more, indicating progressively weaker metal–metal interaction with increasing separation.[71–85] Importantly, **1** was isolated in high purity of a single geometrical isomer (Fig. 1).[73] Compound **1** was also chosen for this investigation because it contains the prototype cyclometalating ligand, C-deprotonated 2-phenylpyridine (ppy),[73] to enable direct comparison to benchmark compounds having the same ligand. Mononuclear complexes featuring this chromophoric ligand, such as Pt(ppy)$_2$[38,89] and Pt(ppy)(acac),[39,90] typically emit green light that is highly structured consistent with their classification as LC transitions with modest admixture of MLCT character. Relative to the green photoluminescence of these mononuclear Pt(II) complexes comprising the ppy ligand, the emission spectrum of **1** was dramatically red-shifted (λ_{max} 726 nm in THF at 295 K, and 685 nm in 2-methyl-THF glass at 77 K), and was broad and featureless in accord with the assignment of MMLCT character (Fig. 2).[73] The broad S_0 to S_1 absorption at 508 nm (Fig. 2) was previously assigned as being MMLCT in nature.[73]

Intricate details of the emissive triplet state from metal complexes have been elucidated through photophysical measurements at temperatures down to T = 1.7 K.[6,40–43,55–61,67,89,90] The zero-field splitting among the three sublevels of the triplet state and their individual decay rates depend upon the strength of the spin–orbit coupling (SOC) interaction. The SOC in turn is dependent upon the degree of metal orbital character involved in the transition (*e.g.* MLCT character) because the SOC constants for heavy atoms such as 3rd row transition metals (ζ(Pt) = 4481 cm^{-1}; ζ(Ir) = 3909 cm^{-1})[91] are so much larger than those of lighter elements present in the ligands. Yersin and co-workers have developed a classification scheme of the nature of the emissive state (*i.e.*, proportion of LC *vs.* MLCT character) based on its ZFS for a large number of mononuclear complexes of second- and third-row d^6 and d^8 metal ions.[42,92–94]

These characteristics of the emissive triplet state have not previously been reported for the intriguing class of dinuclear Pt(II) complexes represented by **1**; these molecules exhibit spectral features and electronic structures that are completely distinct from both the mononuclear Pt(II) complexes and dinuclear Pt(pop) and Pt(pop-BF$_2$). We have therefore undertaken an examination of the photophysical properties of **1** at low temperatures (1.7 to 100 K) in order to determine the ZFS and associated triplet sublevel decay rates.

Experimental

The complex *anti*-[Pt(ppy)(μ-(MepyO))]$_2$, **1**, was synthesized and structurally characterized according to the published procedure.[73] The complex was doped into PMMA by first dissolving 2 mg of **1** in 4 mL methylene chloride in a nitrogen-filled glovebox, and then slowly adding 400 mg of PMMA to make the concentration of the phosphor to 0.5% by weight with respect to the PMMA. The viscous solution of **1** and PMMA was transferred to polyethylene molds placed in a Schlenk apparatus with entry and exit stopcocks attached, and a steady stream of nitrogen was passed through the apparatus to dry the samples followed by further drying under vacuum. For emission measurements in the temperature range of 1.7 to 100 K, a liquid helium cryostat (Cryovac Konti Cryostat IT)

was used in conjunction with a Horiba Jobin Yvon Fluorolog 3 steady-state fluorescence fluorimeter that was modified to additionally enable measurements of emission decay times. As excitation source with the liquid helium cryostat, a PicoQuant LDH-P-C-375 pulsed diode laser (λ_{exc} = 372 nm, pulse width 100 ps) was used. The emission signal was detected with a cooled photomultiplier attached to a FAST ComTec multichannel scalar PCI card with a time resolution of 250 ps. Absolute photoluminescence quantum yield was measured at 77 K with a Hamamatsu C9920-02 system equipped with a Spectralon® integrating sphere. The values for the other temperatures were determined by measuring relative emission intensities and set in relation to the quantum yield value at 77 K.

Results and discussion

Mononuclear, square planar Pt(II) complexes are well-suited to incorporate into Shpol'skii matrices, usually frozen *n*-octane or *n*-nonane.[6,40–43,89,90] These host/guest systems often afford sharp-line emission and excitation spectra at low temperature (<20 K) because the inhomogeneous broadening is extremely small (approximately 1 to 3 cm^{-1}) in the polycrystalline lattice. In many cases, the ZFS can be directly observed in the origin region and vibrational satellites can usually be resolved as well. However, the geometry of **1** makes it unlikely to be amenable to the Shpol'skii technique. Therefore, for this investigation, **1** was doped dilutely (0.5 wt%) into the polymer host, polymethylmethacrylate (PMMA), that has often been used in low-temperature studies of metal complexes.[95,96] The normalized emission spectra measured at 1.7 K and 20 K and the quantum yields determined from 1.7 to 100 K are presented in Fig. 3. Emission spectra for select additional temperatures are shown in Fig. S1 (ESI†). These spectra are broad due to inhomogeneous broadening in the non-crystalline host matrix[97–99] and, as expected for the MMLCT character, coupling to low frequency local phonon modes, M–L vibrations (typically <600 cm^{-1})[92,93,97] and Pt–Pt vibrations of the complex. Although the ZFS cannot be directly resolved in such amorphous hosts because of the inhomogeneous broadening, the ZFS and decay rates of individual sublevels of the emissive triplet state may be obtained by fitting the Boltzmann-type expression (eqn (1)) to the temperature dependence of the observed decay rate at low temperatures ($1.7 < T < 100$ K). This approach echoes the pioneering work of Crosby and co-workers on $Ru(bpy)_3^{2+}$,[95] where k_B is the Boltzmann constant, k_I, k_{II}, and k_{III} are the decay rates of the three individual triplet sublevels, and E_{II} and E_{III} are the zero-field splitting (ZFS) energies of the second and third sublevel, respectively, measured relative to the lowest sublevel.

$$\frac{1}{\tau_{obs}} = k_{obs} = \frac{k_I + k_{II}\exp\left(\frac{-E_{II}}{k_B T}\right) + k_{III}\exp\left(\frac{-E_{III}}{k_B T}\right)}{1 + \exp\left(\frac{-E_{II}}{k_B T}\right) + \exp\left(\frac{-E_{III}}{k_B T}\right)} \quad (1)$$

The observed photoluminescence intensity decays have usually been approximated by a fit of each decay curve to a single-exponential function. However, a consequence of the molecule being doped into the PMMA amorphous host is that the cage environment varies locally, resulting in the inhomogeneous broadening of spectra with a concomitant distribution of intensity decay time constants.[96–100] The approach taken here approximates the distribution of decays for **1** at each temperature by fitting the Kohlrausch–Williams–Watts function,[101–106] eqn (2), also referred to as a stretched exponential, to each decay. The parameter τ in eqn (2) is the decay time corresponding to the maximum amplitude within the distribution of decay times. Values of the parameter β in eqn (2) less than **1** characterize a Lévy distribution of decay rates. When the parameter β is equal to 1, eqn (2) reduces to the familiar single exponential decay. The average decay time (τ_{ave}) is calculated using eqn (3); here, the values of the gamma function, $\Gamma(1/\beta)$, can be readily obtained.[107]

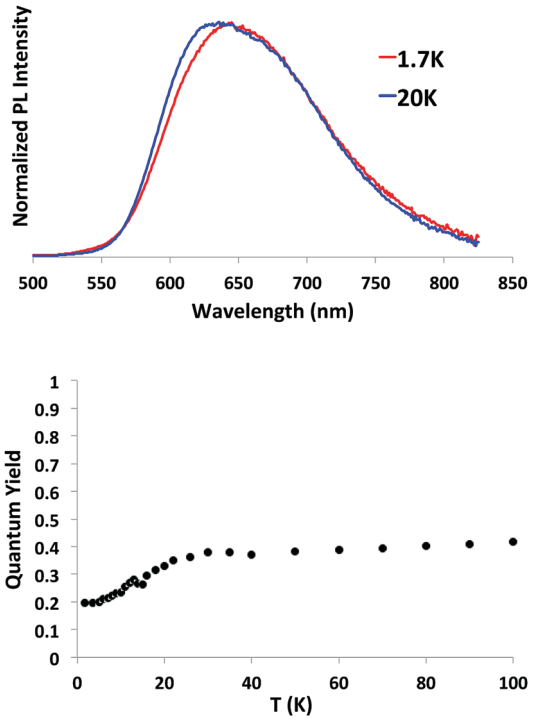

Fig. 3 Top: Normalized emission spectra of **1** in PMMA (0.5 wt%) at 1.7 K and 20 K, 450 nm excitation. Bottom: Temperature dependence of quantum yield of **1** in PMMA host.

$$I = I_0 \exp(-t/\tau)^{\beta} \quad (2)$$

$$\tau_{ave} = (\tau/\beta)\Gamma(1/\beta) \quad (3)$$

$$k_{obs,ave} = 1/\tau_{ave} \quad (4)$$

The photoluminescence intensity decays of **1** recorded over at least five lifetimes at each temperature from 100 K down to 32 K were characterized by values of the parameter β being very close to **1** (0.95 to 0.98), indicating that the emission decay rate from compound **1** was not highly sensitive to local variations in host/guest cage in the PMMA host, although fits to a single exponential were found to be inadequate. By visual inspection of the intensity decay at 32 K plotted on a logarithmic scale (Fig. 4), it is clear that the intensity decay was not far from

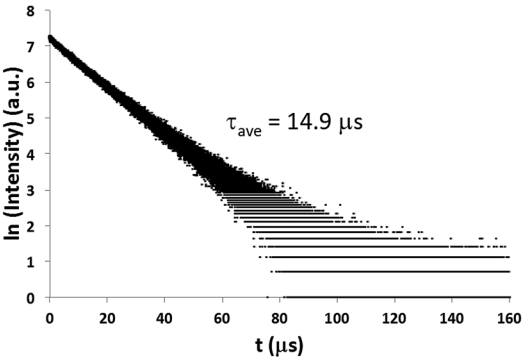

Fig. 4 Logarithmic plot of emission decay of **1** in PMMA (0.5 wt%) at 32 K.

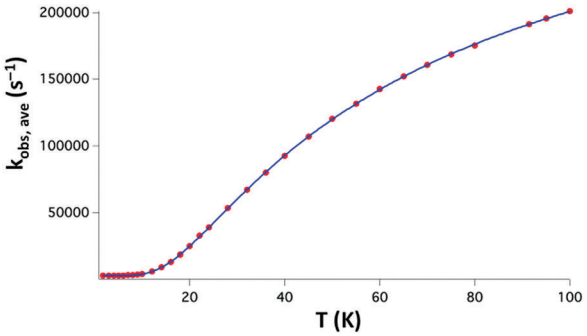

Fig. 6 Temperature dependence of average observed decay rates obtained from fits to the Kohlrausch–Williams–Watts function (eqn (2)–(4)) and the resultant fit (blue solid curve) of the Boltzmann-type expression of eqn (1).

single exponential. As temperature was lowered below 28 K, a distinct short time component became increasingly evident and over this temperature range the overall decay time became increasingly long. The intensity decay at 1.7 K is plotted on a logarithmic scale in Fig. 5. The distinct non-exponential decay at early times arises from something more than simple local variations in the host/guest cage. Possible causes could include spin–lattice relaxation effects, aggregation, or quenching mechanisms. Non-exponential behavior was also reported for Pt(pop) in a frozen glass below 9 K in which the ZFS between one non-degenerate and one doubly degenerate triplet sublevel was found to be 49 cm^{-1}.[55] To obtain the thermalized decay time at these lower temperatures, a visual estimate of the short time component was made and eqn (2) was fit to the portion of the decay at longer times. The point on the decay curve at which the fit to eqn (2) was begun was then iterated two or three times until a value of β (0.91–0.94) was obtained that was close to the values obtained at the higher temperatures in order to include as much of the decay curve in the fit as practical yet exclude most of the impact of the short lifetime component.

The resultant average decay rates from eqn (3) and (4) are shown in Fig. 6. The decay rate at 1.7 K was extremely slow, corresponding to a time constant of 304 μs. This very slow decay was essentially constant over the temperature range from 1.7 to 6 K, above which the rate sharply increased with temperature (Fig. 6). The constant decay rate from 1.7 to 6 K suggests that the upper two sublevels of the triplet manifold, II and III, are frozen out and only the lowest sublevel I emits at these temperatures. The extremely slow decay rate below 6 K also indicates that emission from I is highly forbidden. The photoluminescence emission becomes more allowed at temperatures above 6 K as the higher sublevels become populated. The photoluminescence at 1.7 K also has a lower quantum yield than that at higher temperatures (Fig. 3, bottom). Evidently, the importance of the non-radiative decay rate becomes larger relative to the slow radiative rate of the more forbidden transition. Similar results were observed for $[Ru(bpy)_3^{2+}]$[95] and $Ir(ppy)_3$,[96] the archetypal metal-containing triplet emitters. A clue about the nature of the highly forbidden transition from the lowest sublevel was revealed by comparing the normalized photoluminescence spectrum at 1.7 K, arising only from I, and that at 20 K arising from population of the higher lying sublevels (Fig. 3). The emission spectrum at 20 K was blue-shifted and somewhat wider in band shape than that measured at 2 K. Similar observations have been noted for several Ir(III) complexes in frozen THF and PMMA, albeit more pronounced.[108,109] These observations were interpreted as the level I emission having very little intensity in the origin, being highly forbidden as an electric dipole transition, but gaining intensity in vibrational satellites through a higher-order spin-vibronic coupling; the emission from levels II and III carry significant intensity in their origins in addition to the satellites of totally symmetric modes. Evidence for this mechanism was most clearly observed for mononuclear Pt(II) complexes in Shpol'ski matrices where the sharp-line emission origin for I had practically no intensity and the energy shifts of the vibrational satellites matched certain vibrational frequencies of the complexes, while emission at higher temperatures exhibited origins for levels II and III plus the vibrational satellites in the totally symmetric modes.[40–43] There seems to be at least some involvement of the spin-vibronic coupling in the intensity-gaining mechanism for the transition from the lowest sublevel of **1** as well.

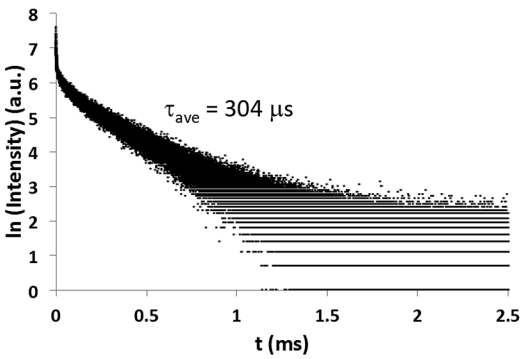

Fig. 5 Logarithmic plot of emission decay of **1** in PMMA (0.5 wt%) at 1.7 K.

The decay temperature dependence data presented in Fig. 6 was first analyzed according to eqn (1). Note that eqn (1) applies whether the MMLCT triplet excited state is delocalized over both halves of the complex, or localized onto one of the ppy ligands. Later, the possibility will be discussed (*vide infra*) whether local variations in the host/guest cage might be large enough to result in the triplet state being localized on one ppy ligand of the dimer having an energy that is significantly

different from that when the triplet is localized on the other ppy ligand such that a population distribution over two triplets having different energies would need to be appropriately modeled.

The value of k_I was taken as the decay rate measured at 1.7 K (1/304 μs = 3.3 ± 0.1 × 10^3 s^{-1}) and used as a fixed parameter in eqn (1). The remaining parameters were then obtained through the fit of eqn (1) to the experimental data (Fig. 6). The ZFS thus obtained were E_{II} = 43 ± 1 cm^{-1} and E_{III} = 150 ± 11 cm^{-1}, while k_{II} was 5.0 ± 0.1 × 10^5 s^{-1} and k_{III} was 5.0 ± 0.2 × 10^5 s^{-1}. The value of the radiative decay rate for *I*, $k_{r,I}$, can be calculated directly from the product of the quantum yield and observed total decay rate at 1.7 K. The values for $k_{r,II}$ and $k_{r,III}$ were then estimated from a fit of the expression in eqn (5) to the quantum yield temperature dependence data:[96]

$$\phi = \frac{k_{r,I} + k_{r,II}\exp\left(-\frac{E_{II}}{k_B T}\right) + k_{r,III}\exp\left(-\frac{E_{III}}{k_B T}\right)}{k_I + k_{II}\exp\left(-\frac{E_{II}}{k_B T}\right) + k_{III}\exp\left(-\frac{E_{III}}{k_B T}\right)} \quad (5)$$

Here, the experimentally determined values for k_I and $k_{r,I}$, and the values of k_{II}, k_{III}, E_{II}, and E_{III} that were obtained from the fit of eqn (1) to the experimental data in Fig. 6 were substituted in eqn (5). The resultant values of $k_{r,I}$, $k_{r,II}$ and $k_{r,III}$ thus obtained were 6.5 ± 0.1 × 10^2, 1.9 ± 0.1 × 10^5 and 3.1 ± 0.2 × 10^5 s^{-1}, respectively. With the respective radiative and observed rates for each sublevel, the quantum yields were calculated as 37 ± 2% and 64 ± 3% for II and III respectively, while the quantum yield of sublevel I already measured as shown in Fig. 3 (bottom) was 20 ± 1%. The values of the photophysical parameters associated with the three triplet sublevels thus obtained are collected in Table 1.

Using a Boltzmann-type expression for the thermal average decay rate, k_{rad}, analogous to eqn (1) and inserting the ZFS and sublevel radiative rates, a value for k_{rad} at 295 K was calculated, the reciprocal of which gave the radiative decay time constant as 7.58 μs. This value is in good agreement with the value of 6.47 μs determined by using the observed decay rate and the quantum yield at 295 K in PMMA, and with the previously determined value of 8.3 μs,[73] albeit in a different environment in solution.

Next, the possibility was considered that in a model of localized excited states the inhomogeneous broadening[96–99] in the PMMA host was so large that it could result in a large difference in the energy of sublevel I localized on one ligand of the di-nuclear complex from that on the other ligand. This implies that a total of six sublevels having all different energies would be involved in the Boltzmann thermal population model for the excited state decay rate. This raises the question of whether the apparent large ZFS determined above could in reality be comprised of two smaller triplet ZFS having different relative energies. Making the matter even more complex, there would be a distribution of the energy differences between the two localized triplets at differing host/guest sites across the sample. This situation would necessarily lead to a broad distribution of decay times if there were a wide distribution of energy differences between the two triplets at different sites. However, this is clearly not the case here, because in the Kohlrausch analysis, the parameter β was found to be very close to unity at all temperatures, experimentally demonstrating that the distribution of observed decay time constants was in fact not very wide. The decay time was essentially constant over the range 1.7 to 6 K, giving no evidence of population of any higher lying sublevel(s) in the corresponding energy range and therefore no evidence for smaller E_{II} values. The overall fit of eqn (1) (Fig. 6) to the data is quantitatively satisfying. Finally, the radiative decay rate predicted for 295 K using the E_i and $k_{r,i}$ values from the low temperature fits was in good agreement with that found experimentally. We therefore find no experimental evidence that local variations in the host/guest cage were strong enough to induce large differences in the electronic origins between MMLCT triplets if they were to be localized on one half of the molecule or the other, at least not for a significant portion of the molecules in the sample. Therefore we favor a model where the fit of the observed intensity decay data by eqn (1) provides the best measure of the ZFS and sublevel decay rates for the emissive state of **1**.

In this regard, it is noted that the temperature dependence of decay rates for other triplet emitters in amorphous hosts, such as $[Ru(bpy)_3]^{2+}$ [95] and $Ir(ppy)_3$,[96,108] have similarly been fit by eqn (1). Moreover, these benchmark triplet emitters have also been examined in single-crystal and polycrystalline hosts. Some differences are of course expected from differences in host environment. Importantly though, the ZFS obtained for amorphous solid matrices by the application of eqn (1) were not very different from those directly observed in the highly resolved spectra in crystalline matrices featuring little inhomogeneous broadening. In the case of $[Ru(bpy)_3]^{2+}$, the ZFS found in PMMA by fitting eqn (1) to the measured decay rates[95] was almost the same as was found in high-resolution, experiments applying crystalline matrices.[110,111] We analyzed decays of this archetypal emitter having significant MLCT character in PMMA (0.5 wt%) as a comparison and found values of the Kohlrausch parameter β between 0.95 and 0.96 from 77 K to 200 K, very similar to values reported above for 1. For $Ir(ppy)_3$, E_{III} was estimated to vary over a range between 114 to 135 cm^{-1} in PMMA by separately fitting short and long time components of the intensity decays by eqn (1), while the ZFS of the dominant site in frozen polycrystalline CH_2Cl_2 was found to be 170 cm^{-1} in highly resolved spectra.[96] The ZFS of Pt(pop) (~41 cm^{-1}) showed no significant differences in a glassy matrix or in various crystalline forms.[56]

The total ZFS for **1** (150 cm^{-1}) is significantly larger than those found for mononuclear Pt(II) cyclometalates involving ppy (32 cm^{-1} for $Pt(ppy)_2$;[89] 11.5 cm^{-1} for Pt(ppy)(acac);[90] 23 cm^{-1} for a tetradentate complex comprising two covalently linked ppy units.[6]) The emissive states of the cited literature Pt(II)

Table 1 Values of E_i, k_i, $k_{r,i}$ and ϕ_i for the *i*th triplet sublevel of **1** obtained from application of eqn (1)–(5)

*i*th sublevel	E_i (cm^{-1})	k_i (s^{-1})	$k_{r,i}$ (s^{-1})	ϕ_i (%)
I	0	3.3 ± 0.1 × 10^3	6.5 ± 0.1 × 10^2	20 ± 1
II	43 ± 1	5.0 ± 0.1 × 10^5	1.9 ± 0.1 × 10^5	37 ± 2
III	150 ± 11	5.0 ± 0.2 × 10^5	3.1 ± 0.2 × 10^5	64 ± 3

cyclometalates have been assigned as mainly LC with a moderate admixture of MLCT character based on the vibronic structure of the respective emission spectra, the low extinction coefficient of the resolved S_0 to T_1 absorption, and the moderate ZFS. The larger ZFS of **1** provided experimental evidence that its emissive state has much more metal orbital character, consistent with the earlier assignment[73] as a MMLCT transition arising from the d_{z^2} σ^* HOMO. This large ZFS places **1** among complexes of other 3rd row metals exhibiting the largest reported values of ZFS. The deep red MLCT emitter $Os(bpy)_3^{2+}$ exhibited a E_{III} in single-crystal hosts of 211 cm^{-1}.[112–114] As already mentioned, $Ir(ppy)_3$ was found to have an E_{III} of 170 cm^{-1} in frozen CH_2Cl_2, and somewhat smaller values in frozen THF or PMMA.[96] ZFS of a large number of other d^6 and d^8 metal complexes have been tabulated.[93,94]

The high degree of metal orbital participation in the MMLCT excited state indicated by the large ZFS raises the question whether the coupling through the σ^* (d_{z^2}) orbital could be greater than the localization energy from variations in the host/guest cage, resulting in the emissive state being delocalized over both halves of the molecule. The data do not allow us to distinguish whether the triplet excited state is delocalized over both halves of the molecule, or localized to one half of the molecule. We note that corresponding investigations have been carried out for $Ru(bpy)_3^{2+}$ and $Os(bpy)_3^{2+}$ using heteroleptic compounds with deuterated and protonated ligands, respectively, to address this question.[110,113] But if the localized situation is realized, then according to the preceding analysis, it may be concluded that, relative to the ZFS, there are not significant differences in energy of the triplet localized onto the second half compared to that on the first arising from local variation in environment.

In Pt(pop) and Pt(pop-BF_2), the lowest energy excited states, S_1 and T_1, have been assigned to σ^* (d_{z^2}) $\rightarrow$ σ (p_z) transitions within the Pt–Pt core. In these high-symmetry (approximate D_{4h}) dinuclear complexes, the lowest triplet splits into a non-degenerate sublevel and a two-fold degenerate sublevel with ZFS of 40 to 50 cm^{-1}.[55–57,67] The Boltzmann distribution according to this model having one non-degenerate and one doubly degenerate sublevel did not provide a good fit to the experimental decay temperature dependence for **1**.

The spectral and photophysical properties of **1** are distinct from those of Pt(pop) and Pt(pop-BF_2) in other ways as well. The most unusual property of the latter complexes was that the intersystem crossing rate between S_1 and T_1 was extremely slow, resulting in both fluorescence and phosphorescence. But there was no indication of such slow ISC in **1**. The $S_0 \rightarrow S_1$ and $S_0 \rightarrow T_1$ absorption bands of Pt(pop) and Pt(pop-BF_2), both of σ^* (d_{z^2}) $\rightarrow$ σ(p_z) parentage, were well-separated and the S_1–T_1 energy gap can be estimated from the respective λ_{max} to be 5124 cm^{-1} for Pt(pop)[54] and 5370 cm^{-1} for Pt(pop-BF_2).[66] The corresponding emission bands were well-separated as well and lead to similar estimates for S_1–T_1. In contrast, the $S_0 \rightarrow T_1$ absorption was not resolved for **1** (Fig. 2).[73] Although this suggests a smaller S_1–T_1 gap, it cannot be directly estimated. But the apparent Stokes shifts from the $S_0 \rightarrow S_1$ absorption λ_{max} to the $S_0 \rightarrow T_1$ emission λ_{max} may be compared. The Stokes shift for **1** in solution[73] was 5911 cm^{-1}, whereas it was 7906 cm^{-1} for Pt(pop)[54] and 7866 cm^{-1} Pt(pop-BF_2).[66] These values suggest that the S_1–T_1 gap was about 2000 cm^{-1} smaller for **1** than for the latter two complexes. A small S_1–T_1 gap is consistent with the assignment as a type of charge transfer transition.[115]

However, Pt(pop), Pt(pop-BF_2), and **1** do share a striking commonality in the degree to which emission from sublevel I was so highly forbidden with radiative decay times estimated as 1.7,[55] 8.6,[67] and 1.5 ms, respectively. Among mononuclear Pt(II) and Ir(III) complexes, only those that were classified as highly LC exhibited values even close to these long lifetimes.[93,94]

According to the published empirical correlation between ZFS and radiative lifetime developed for mononuclear d^6 and d^8 emitters of the LC/MLCT type,[92–94] a total ZFS splitting as large as 150 cm^{-1} would predict a radiative lifetime at 300 K of about 1.5 to 2 μs, whereas the calculated value for **1** using the ZFS and decay rates determined here was about 7.6 μs. In the case of Pt(pop-BF_2), the total ZFS of 40 cm^{-1} would lead to a prediction of about 2 to 3 μs for k_{rad} at 300 K, whereas we calculate a value of 7.2 μs using the published ZFS and sublevel decay rates.[67] It must be emphasized, however, that no analytical expression relates the ZFS to the radiative decay rate because the later depends only upon SOC to singlet states, while the former includes SOC and configuration interaction to higher lying triplet states.[93,94,116] We believe that the different relation between ZFS and decay time reported here for **1** reflects upon the unique geometry and consequently different details of electronic structure and SOC pathways in the distinct class of emitters represented by **1**.

Conclusions

A representative of a class of dinuclear, cyclometalated Pt complexes featuring MMLCT emission was examined for the first time by low temperature emission decay kinetics (1.7 K < T < 100 K). Analysis of the photoluminescence intensity decays of the complex doped into a polymer host by the Kohlrausch–Williams–Watts function revealed small deviations from single-exponential decay. It was concluded that the polymer induces only a moderate distribution of emission decay times due to local variations in the host/guest cage. The temperature dependence of the average decay times was modeled well by a Boltzmann-type expression for one emissive triplet state. The resultant total ZFS was large (150 cm^{-1}) due to the high degree of metal-orbital participation in the transition. Photoluminescence emission from the lowest triplet sublevel was unusually strongly forbidden with a radiative decay constant of approximately 1.5 ms. The combined data illustrate the importance of determining these low temperature photophysical properties and ZFS parameters in order to reveal the nature and the degree of metal orbital participation in these excited states. Future experimentation on related dimeric structures with systematic variation in geometry (metal–metal angular overlap in particular) and chromophoric ligand will likely reveal more details regarding the Pt–Pt and the

Pt-ligand interactions that ultimately control the photophysical and photochemical properties of these molecules.

Conflicts of interest

There are no conflicts to declare.

Acknowledgements

The authors thank Mr Alexander Schinabeck, Institut für Physikalische Chemie, Universität Regensburg, for technical assistance with the low temperature experiments. This work was supported by the National Science Foundation under Award CHE-1665033.

Notes and references

1 B. Ma, P. I. Djurovich, S. Garon, B. Alleyne and M. E. Thompson, *Adv. Mater.*, 2006, **16**, 2438–2446.
2 H. F. Xiang, S. W. Lai, P. T. Lai and C.-M. Che in *Highly Efficient OLEDs with Phosphorescent Materials*, ed. H. Yersin, Wiley-VCH, Weinheim, Germany, 2007.
3 J. A. G. Williams in *Topics in Organometallic Chemistry*, ed. H. Bozec and V. Guerchais, Springer, New York, 2009.
4 E. Turner, N. Bakken and J. Li, *Inorg. Chem.*, 2013, **52**, 7344–7351.
5 T. Fleetham, J. Ecton, Z. Wang, N. Bakken and J. Li, *Adv. Mater.*, 2013, **25**, 2573–2576.
6 D. A. K. Vezzu, J. C. Deaton, S. J. Jones, L. Bartolotti, C. F. Harris, A. P. Marchetti, M. Kondakova, R. D. Pike and S. Huo, *Inorg. Chem.*, 2010, **49**, 5107–5119.
7 P.-K. Chow, G. Cheng, G. S. M. Tong, W.-P. To, W. L. Kwong, K.-H. Low, C.-C. Kwok, C. Ma and C.-M. Che, *Angew. Chem., Int. Ed.*, 2015, **54**, 2084.
8 K. M.-C. Wong, M.-C. Tang, Y.-C. Wong, M. Ng, M.-Y. Chan and V. W.-W. Yam, *J. Am. Chem. Soc.*, 2017, **139**, 6351–6362.
9 K. M.-C. Wong and V. W.-W. Yam, *Coord. Chem. Rev.*, 2007, **251**, 2477–2488.
10 D. S.-H. Chan, H. M. Lee, C.-M. Che, C. H. Leung and D. L. Ma, *Chem. Commun.*, 2009, 7479–7481.
11 B. Y. W. Man, D. S.-H. Chan, H. Yang, S. W. Ang, F. Yang, S. C. Yan, C. M. Ho, P. Wu, C.-M. Che, C. H. Leung and D. L. Ma, *Chem. Commun.*, 2010, **46**, 8534–8536.
12 H. Guo, S. Ji, W. Wu, J. Shao and J. Zhao, *Analyst*, 2010, **135**, 2832–2840.
13 S. M. Drew, D. E. Janzen, C. E. Buss, D. I. MacEwan, K. M. Dublin and K. R. Mann, *J. Am. Chem. Soc.*, 2001, **123**, 8414–8415.
14 S. M. Drew, D. E. Janzen and K. R. Mann, *Anal. Chem.*, 2002, **74**, 2547–2555.
15 S. M. Drew, L. I. Smith, K. A. McGhee and K. R. Mann, *Chem. Mater.*, 2009, **21**, 3117–3124.
16 M. J. Cich, I. M. Hill, A. D. Lackner, R. J. Martinez, T. C. Ruthenburg, Y. Takeshita, A. J. Young, S. M. Drew, C. E. Buss, D. I. MacEwan and K. R. Mann, *Sens. Actuators, B*, 2010, **149**, 199–204.
17 P. Wu, E. L. M. Wong, D. L. Ma, G. S. M. Tong, K. M. Ng and C.-M. Che, *Chem. – Eur. J.*, 2011, **17**, 4109–4112.
18 H. S. Lo, S. K. Yip, K. M.-C. Wong, N. Zhu and V. W.-W. Yam, *Organometallics*, 2006, **25**, 3537–3540.
19 Q.-Z. Yang, L.-Z. Wu, H. Zhang, B. Chen, Z.-X. Wu, L.-P. Zhang and C.-H. Tung, *Inorg. Chem.*, 2004, **43**, 5195–5197.
20 A. M. Prokhorov, T. Hofbeck, R. Czerwieniec, A. F. Suleymanova, D. N. Kozhevnikov and H. Yersin, *J. Am. Chem. Soc.*, 2014, **136**, 9637–9642.
21 E. C.-H. Kwok, M.-Y. Chan, K. M.-C. Wong, W. H. Lam and V. W.-W. Yam, *Chem. – Eur. J.*, 2010, **16**, 12244–12254.
22 F. Gui, K. Ogawa, Y.-G. Kim, E. O. Danilov, F. N. Castellano, J. R. Reynolds and K. S. Schanze, *Phys. Chem. Chem. Phys.*, 2007, **9**, 2724–2734.
23 Y. Zhang, H. Zhang, X. Mu, S.-W. Lai, B. Xu, W. Tian, Y. Wang and C.-M. Che, *Chem. Commun.*, 2010, **46**, 7727–7729.
24 T. N. Singh-Rachford and F. N. Castellano, *Inorg. Chem.*, 2009, **48**, 2541–2548.
25 J.-H. Kim, F. Deng, F. N. Castellano and J.-H. Kim, *ACS Photonics*, 2014, **1**, 382–388.
26 D. Zhang, L.-Z. Wu, L. Zhou, X. Han, Q.-Z. Yang, L.-P. Zhang and C.-H. Tung, *J. Am. Chem. Soc.*, 2004, **126**, 3440–3441.
27 R. Narayana-Prabhu and R. H. Schmehl, *Inorg. Chem.*, 2006, **45**, 4319–4321.
28 P. Du, J. Schneider, P. Jarosz and R. Eisenberg, *J. Am. Chem. Soc.*, 2006, **128**, 7726–7727.
29 P. Du, J. Schneider, P. Jarosz, J. Zhang, W. W. Brennessel and R. Eisenberg, *J. Phys. Chem. B*, 2007, **111**, 6887–6894.
30 P. Du, K. Knowles and R. Eisenberg, *J. Am. Chem. Soc.*, 2008, **130**, 12576–12577.
31 K. Feng, R. Y. Zhang, L.-Z. Wu, B. Tu, M.-L. Peng, L.-P. Zhang, D. Zhao and C.-H. Tung, *J. Am. Chem. Soc.*, 2006, **128**, 14685–14690.
32 J.-J. Zhong, Q.-Y. Meng, G.-X. Wang, Q. Liu, B. Chen, K. Feng, C.-H. Tung and L.-Z. Wu, *Chem. – Eur. J.*, 2013, **19**, 6443–6450.
33 P. Wu, E. L. M. Wong, D. L. Ma, G. S. M. Tong, K. M. Ng and C.-M. Che, *Chem. – Eur. J.*, 2009, **15**, 3652–3656.
34 K. M.-C. Wong, W.-S. Tang, B. W. K. Chu, N. Zhu and V. W.-W. Yam, *Organometallics*, 2004, **23**, 3459–3465.
35 D. Septiadi, A. Aliprandi, M. Mauro and L. De Cola, *RSC Adv.*, 2014, **4**, 25709–25718.
36 R. Y. W. Sun, A. L. F. Chow, X. H. Li, J. J. Yan, S. S. Y. Chui and C.-M. Che, *Chem. Sci.*, 2011, **2**, 728–736.
37 V. W.-W. Yam, V. K.-M. Au and S. Y.-L. Leung, *Chem. Rev.*, 2015, **115**, 7589–7728.
38 L. Chassot, E. Müller and A. von Zelewsky, *Inorg. Chem.*, 1984, **23**, 4249–4253.
39 J. Brooks, Y. Babayan, S. Lamansky, P. I. Djurovich, I. Tsyba, R. Bau and M. E. Thompson, *Inorg. Chem.*, 2002, **41**, 3055–3066.
40 H. Wiedenhofer, S. Schutzenmeier, A. von Zelewsky and H. Yersin, *J. Phys. Chem.*, 1995, **99**, 13385–13391.

41 J. Schmidt, H. Wiedenhofer, A. von Zelewsky and H. Yersin, *J. Phys. Chem.*, 1995, **99**, 226–229.
42 H. Yersin and D. Donges, *Top. Curr. Chem.*, 2001, **214**, 81–186.
43 A. F. Rausch and H. Yersin, *Chem. Phys. Lett.*, 2010, **484**, 261–265.
44 K.-W. A. Chan, M. Ng, Y.-C. Wong, M.-Y. Chan, W.-T. Wong and V. W.-W. Yam, *J. Am. Chem. Soc.*, 2017, **139**, 10750–10761.
45 C. W. Chan, L. K. Cheng and C.-M. Che, *Coord. Chem. Rev.*, 1994, **132**, 87–97.
46 M. Hissler, W. B. Connick, D. K. Gieger, J. E. McGarrah, D. Lipa, R. J. Lachicotte and R. Eisenberg, *Inorg. Chem.*, 2000, **39**, 447–457.
47 C. E. Whittle, J. A. Weinstein, M. W. George and K. S. Schanze, *Inorg. Chem.*, 2001, **40**, 4053–4062.
48 F. N. Castellano, I. E. Pomestchenko, E. Shikova, F. Hua, M. Muro and M. N. Rajapakse, *Coord. Chem. Rev.*, 2006, **250**, 1819–1828.
49 F. Hua, S. Kinayyigit, J. Cable and F. N. Castellano, *Inorg. Chem.*, 2006, **45**, 4304–4305.
50 A. A. Rachford, F. Hua, C. J. Adams and F. N. Castellano, *Dalton Trans.*, 2009, 3950–3954.
51 R. Liu, Y. Li, Y. Li, H. Zhu and W. Sun, *J. Phys. Chem. A*, 2010, **114**, 12639–12645.
52 M. Bachmann, D. Suter, O. Blacque and K. Venkatesan, *Inorg. Chem.*, 2016, **55**, 4733–4745.
53 R. P. Sperline, M. K. Dickson and D. M. Roundhill, *J. Chem. Soc., Chem. Commun.*, 1977, 62–63.
54 C.-M. Che, L. G. Butler and H. B. Gray, *J. Am. Chem. Soc.*, 1981, **103**, 7796–7797.
55 W. A. Fordyce, J. G. Brummer and G. A. Crosby, *J. Am. Chem. Soc.*, 1981, **103**, 7061–7064.
56 J. T. Markert, D. P. Clements, M. R. Corson and J. K. Nagle, *Chem. Phys. Lett.*, 1983, **97**, 175–179.
57 S. F. Rice and H. B. Gray, *J. Am. Chem. Soc.*, 1983, **105**, 4571–4575.
58 A. E. Stiegman, S. F. Rice, H. B. Gray and V. M. Miskowski, *Inorg. Chem.*, 1987, **26**, 1112–1116.
59 L. Bär, H. Englmeier, G. Gliemann, U. Klement and K.-J. Range, *Inorg. Chem.*, 1990, **29**, 1162–1168.
60 Y. Shimizu, Y. Tanaka and T. Azumi, *J. Phys. Chem.*, 1985, **89**, 1372–1374.
61 Y. Tanaka and T. Azumi, *Inorg. Chem.*, 1986, **25**, 247–248.
62 Y. Shimizu, Y. Tanaka and T. Azumi, *J. Phys. Chem.*, 1984, **88**, 2423–2425.
63 C.-M. Che, L. G. Butler, H. B. Gray, R. M. Crooks and W. H. Woodruff, *J. Am. Chem. Soc.*, 1983, **105**, 5492–5494.
64 W. B. Heuer, M. D. Totten, G. S. Rodman, E. J. Hebert, H. J. Tracy and J. K. Nagle, *J. Am. Chem. Soc.*, 1984, **106**, 1163–1164.
65 R. M. van der Veen, A. Cannizzo, F. van Mourik, A. Vlček, Jr. and M. Chergui, *J. Am. Chem. Soc.*, 2011, **133**, 305–315.
66 A. C. Durrell, G. E. Keller, Y.-C. Lam, J. Sýkora, A. Vlček, Jr. and H. B. Gray, *J. Am. Chem. Soc.*, 2012, **134**, 14201–14207.
67 T. Hofbeck, Y.-C. Lam, M. Kalbáč, S. Záliš, A. Vlček, Jr. and H. Yersin, *Inorg. Chem.*, 2016, **55**, 2441–2449.
68 Y.-C. Lam, H. B. Gray and J. R. Winkler, *J. Phys. Chem. A*, 2016, **120**, 7671–7676.
69 R. M. van der Veen, C. J. Milne, A. El Nahhas, F. A. Lima, V.-T. Pham, J. Best, J. A. Weinstein, C. N. Borca, R. Abela, C. Bressler and M. Chergui, *Angew. Chem., Int. Ed.*, 2009, **48**, 2711–2714.
70 I. Novozhilova, A. Volkov and P. J. Coppens, *J. Am. Chem. Soc.*, 2003, **125**, 1079–1087.
71 B. Ma, J. Li, P. I. Djurovich, M. Yousufuddin, R. Bau and M. E. Thompson, *J. Am. Chem. Soc.*, 2005, **127**, 28–29.
72 A. Chakraborty, J. C. Deaton, A. Haefele and F. N. Castellano, *Organometallics*, 2013, **32**, 3819–3829.
73 A. Chakraborty, J. E. Yarnell, R. D. Sommer, S. Roy and F. N. Castellano, *Inorg. Chem.*, 2018, **57**, 1298–1310.
74 C. E. McCusker, A. Chakraborty and F. N. Castellano, *J. Phys. Chem. A*, 2014, **118**, 10391–10399.
75 S. Akatsu, Y. Kanematsu, T. Kurihara, S. Sueyoshi, Y. Arikawa, M. Onishi, S. Ishizaka, N. Kitamura, Y. Nakao and S. Sakaki, *et al.*, *Inorg. Chem.*, 2012, **51**, 7977–7992.
76 C. Zhou, L. Yuan, Z. Yuan, N. K. Doyle, T. Dilbeck, D. Bahadur, S. Ramakrishnan, A. Dearden, C. Huang and B. Ma, *Inorg. Chem.*, 2016, **55**, 8564–8569.
77 S.-W. Lai, M. C.-W. Chan, T. C. Cheung, S.-M. Peng and C.-M. Che, *Inorg. Chem.*, 1999, **38**, 4046–4055.
78 S.-W. Lai, M. C. W. Chan, K.-K. Cheung, S.-M. Peng and C.-M. Che, *Organometallics*, 1999, **18**, 3991–3997.
79 T. Koshiyama, A. Omura and M. Kato, *Chem. Lett.*, 2004, **33**, 1386–1387.
80 M. Yoshida, N. Yashiro, H. Shitama, A. Kobayashi and M. Kato, *Chem. – Eur. J.*, 2016, **22**, 491–495.
81 V. Sicilia, P. Borja and A. Martín, *Inorganics*, 2014, **2**, 508–523.
82 R. Aoki, A. Kobayashi, H.-C. Chang and M. Kato, *Bull. Chem. Soc. Jpn.*, 2011, **84**, 218–225.
83 E. A. Katlenok, A. A. Zolotarev, A. Y. Ivanov, S. N. Smirnov and K. P. Balashev, *J. Struct. Chem.*, 2015, **56**, 880–886.
84 M. A. Bennett, S. K. Bhargava, E. C. Cheng, W. H. Lam, T. K. Lee, S. H. Privér, J. Wagler, A. C. Willis and V. W. W. Yam, *J. Am. Chem. Soc.*, 2010, **132**, 7094–7103.
85 V. Sicilia, J. Forniés, J. M. Casas, A. Martín, J. A. López, J. A. Larraz, P. Borja, C. Ovejero, D. Tordera and H. Bolink, *Inorg. Chem.*, 2012, **51**, 3427–3435.
86 J. V. Lockard, A. A. Rachford, G. Smolentsev, A. B. Stickrath, X. Wang, X. Zhang, K. Atenkoffer, G. Jennings, A. Soldatov and A. L. Rheingold, *et al.*, *J. Phys. Chem. A*, 2010, **114**, 12780–12787.
87 K. Haldrup, A. O. Dohn, M. L. Shelby, M. W. Mara, A. B. Stickrath, M. R. Harpham, J. Huang, X. Zhang, K. B. Møller and A. Chakraborty, *et al.*, *J. Phys. Chem. A*, 2016, **120**, 7475–7483.
88 P. Kim, M. S. Kelley, A. Chakraborty, N. L. Wong, R. P. Van Duyne, G. C. Schatz, F. N. Castellano and L. X. Chen, *J. Phys. Chem. C*, 2018, **122**, 14195–14204.
89 J. Strasser, H. H. H. Homeier and H. Yersin, *Chem. Phys.*, 2000, **255**, 301–316.
90 A. Rausch, PhD thesis, Universitat Regensburg, 2011.

91 M. Montalti, A. Credi, L. Prodi and M. T. Gandolfi, *Handbook of Photochemistry*, Taylor and Francis, Boca Raton, Florida, 3rd edn, 2006.
92 H. Yersin and W. Finkenzeller, in *Highly efficient OLEDs with Phosphorescent Materials*, ed. H. Yersin, Wiley-VCH Verlag GmbH & Co. KGaA, Weinheim, 2008, p. 39.
93 H. Yersin, A. F. Rausch and R. Czerwieniec, in *Physics of Organic Semiconductors*, ed. W. Brutting and C. Adachi, Wiley-VCH Verlag GmbH & Co. KGaA, Weinheim, 2nd edn, 2012.
94 H. Yersin, A. F. Rausch, R. Czerwieniec, T. Hofbeck and T. Fischer, *Coord. Chem. Rev.*, 2011, **255**, 2622–2652.
95 G. D. Hager and G. A. Crosby, *J. Am. Chem. Soc.*, 1975, **97**, 7031–7037.
96 T. Hofbeck and H. Yersin, *Inorg. Chem.*, 2010, **49**, 9290–9299.
97 M. Colombo, A. Hauser and H. U. Güdel, *Top. Curr. Chem.*, 1994, **171**, 144–171.
98 E. Krausz, J. Higgins and H. Riesen, *Inorg. Chem.*, 1993, **32**, 4053–4056.
99 R. Bauer, W. Finkenzeller, U. Bogner, M. E. Thompson and H. Yersin, *Org. Electron.*, 2008, **9**, 641–648.
100 A. F. Rausch, M. E. Thompson and H. Yersin, *Inorg. Chem.*, 2009, **48**, 1928–1937.
101 R. Kohlrausch, *Ann. Phys. Chem.*, 1854, **91**, 179–214.
102 G. Williams and D. C. Watts, *Trans. Faraday Soc.*, 1970, **66**, 80–85.
103 M. N. Berberan-Santos, E. N. Bodunov and B. Valeur, *Chem. Phys.*, 2005, **315**, 171–182.
104 D. W. Thompson, C. N. Fleming, B. D. Myron and T. J. Meyer, *J. Phys. Chem. B*, 2007, **111**, 6930–6941.
105 M. M. McGoorty, R. S. Khnayzer and F. N. Castellano, *Chem. Commun.*, 2016, **52**, 7846–7849.
106 F. N. Castellano, T. A. Heimer, M. T. Tandhasetti and G. J. Meyer, *Chem. Mater.*, 1994, **6**, 1041–1048.
107 Definition of the gamma function and a convenient on-line calculator may be found at www.medcalc.org.
108 W. J. Finkenzeller and H. Yersin, *Chem. Phys. Lett.*, 2003, **377**, 299–305.
109 J. C. Deaton, R. H. Young, J. R. Lenhard, M. Rajeswaran and S. Huo, *Inorg. Chem.*, 2010, **49**, 9151–9161.
110 H. Yersin, W. Humbs and J. Strasser, *Top. Curr. Chem.*, 1997, **191**, 153–249.
111 H. Riesen, L. Wallace and E. Krausz, *Chem. Phys. Lett.*, 1994, **228**, 605–609.
112 H. Yersin, E. Gallhuber and G. Hensler, *Chem. Phys. Lett.*, 1987, **140**, 157–162.
113 P. Huber and H. Yersin, *J. Phys. Chem.*, 1993, **97**, 12705–12709.
114 H. Yersin, E. Gallhuber and G. Hensler, *Chem. Phys. Lett.*, 1987, **140**, 157–162.
115 H. Yersin, *Top. Curr. Chem.*, 2004, **241**, 1–26.
116 ''Archetypal Iridium(III) Compounds for Optoelectronic and Photonic Applications: Photophyscial Properties and Synthetic Methods'', J. C. Deaton and F. N. Castellano, in *Iridium(III) in Optoelectronic and Photonic Applications*, ed. Zysman-Colman, E., Wiley, 2017.

